EAI Endorsed Transactions
on Energy Web

Research Article EAI.EU

Optimization Design of Surface-mounted Permanent Magnet Synchronous Motors Using Genetic Algorithms

Trinh Truong Cong[1], Thanh Nguyen Vu[1,*], Gabriel Pinto[2] and Vuong Dang Quoc[1]

[1]Laboratory of High-Performance Electric Machines (HiPems); School of Electrical and Electronic Engineering; Hanoi University of Science and Technology, No1, Dai Co Viet street, Hai Ba Trung District, Hanoi, Viet Nam
[2]Universidade do Minho - Departamento de Eletrónica Industrial (DEI), Campus de Azurém - 4800-058 Guimarães, Portugal

Abstract

The permanent magnet synchronous motor (PMSM) has gained widespread popularity in various industrial applications due to its simple structure, reliable performance, compact size, high efficiency, and adaptability to different shapes and sizes. Its exceptional characteristics have made it a focal point in industrial settings. The PMSM can be categorized into two primary types based on the arrangement of the permanent magnets (PM): interior permanent magnet (IPM) and surface-mounted permanent magnet (SPM). In the IPM, the magnets are embedded into the rotor, while in SPM, they are mounted on the rotor's surface. The utilization of PMs eliminates the need for excitation currents due to their high flux density and significant coercive force. This absence of excitation losses contributes to a notable increase in efficiency. In this study, a multi-objective optimal design approach is introduced for a surface mounted PMSM, aiming to achieve maximum efficiency while minimizing material costs. The optimization task is accomplished using a genetic algorithm. Furthermore, the motor designs are simulated using the finite element method (FEM) to assess and compare designs before and after the optimization process.

Keywords: Permanent magnet synchronous motor (PMSM), Surface-mounted permanent magnet synchronous motor (SPMSM), genetic algorithm (GA), finite element method

Received on 10 November 2023, accepted on 08 January 2024, published on 16 January 2024

doi: 10.4108/ew.4864

*Corresponding author. Email: thanh.nguyenvu@hust.edu.vn

1. Introduction

The permanent magent synchronous motor (PMSM) is widely employed in diverse industrial applications due to its simplicity, reliability, compact size, high efficiency, and its ability to be adapted to various shapes and sizes [1]. Particularly, in the low speed, the PMSMs have extensive usage in fields such as ship propulsion, lifting, mining, and oil field exploitation [2], [3]. The PMSMs can be classified into two main types based on the arrangement of the permanent magnet: interior permanent magnet (IPM), where the magnets are embedded into the rotor, and surface-mounted permanent magnet (SPM), where the magnets are mounted on the rotor's surface. The PMSMs are excited by permanent magnets (PMs) rather than excitation currents due to their high flux density and significant coercive force. This characteristic eliminates excitation losses, resulting in a substantial increase in efficiency [4]. The three primary magnet materials used in the PMSMs are ferrite, samarium-cobalt (SmCo), and neodymium-iron-boron (NdFeB).

For high-torque applications, the fractional-slot concentrated winding is commonly employed. The term fractional-slot winding refers to a situation where the number of slots per pole per phase is a non-integer value and less than one. When each coil of the winding is wound around a single tooth of the stator, it is referred to as a concentrated winding. Motors with this type of winding are particularly advantageous in low-speed direct drive transmission systems due to their high efficiency, reduced end turn length, high slot fill factor, and low copper loss. However, fractional-slot configurations have drawbacks, including slightly lower winding factor and higher harmonic content in the magnetomotive force (MMF), distribution compared to integral slot machines [5], [6]. Therefore, the motor must be designed with a suitable combination of the number of pole pairs and slots based on its intended applications.

The genetic algorithm (GA) is an heuristic search frequently employed for generating effective solutions to optimization and search problems. Inspired by natural evolution, the GA utilizes techniques such as inheritance, mutation, selection, and crossover to generate solutions for optimization problems. Its versatility makes it a powerful tool for global optimization and analysis of large datasets [7]. Numerous researchers have utilized the genetic algorithm to explore optimal designs for the PMSMs [8]-[10]. However, the discrete variation of variables and their lack of complete correlation with each other and other parameters can lead to changes in output power after the optimization process.

In this study, a surface-mounted permanent magnet synchronous motor (SPMSM) employing NdFeB N35 magnets is designed. Subsequently, the genetic algorithm is applied to determine the optimal dimensions that achieve maximum efficiency while minimizing material costs (such as electrical steel, copper, and magnets) with power conservation.

2. Analytical model of SPMSM

The rotor volume, expressed as the product of D^2 and L, plays a crucial role in determining the motor's dimensions, where D represents the inner diameter of the stator and L denotes the active length of the machine. Several methods have been proposed to calculate this parameter [11]-[13]. However, to determine the rotor volume, a coefficient concept that depends on the cooling systems, as presented in [14], is employed.

$$\frac{D^2L}{T_e} = V_o, \tag{1}$$

where T_e is the motor torque.

Typically, for motors with an output power of up to 10 hp and air cooling, the specific volume (V_0) ranges from 5 to 7 in^3/(ft·lb). On the other hand, for motors with a power greater than 10 hp and water or liquid cooling, the specific volume is typically between 2 and 5 in^3/(ft·lb).

The magnet is a critical component of the PMSM, as it generates the magnetic field in the air gap. In this paper, NdFeB N35 magnets are utilized. The fundamental flux density in the air gap can be determined using the following equation:

$$B_g = \frac{4}{\pi} sin\left(\frac{\rho_{pm}}{2}\right) B_m, \tag{2}$$

where ρ_{pm} represents the electrical angle of the PM, and B_m is the flux density of the magnet. The thickness of magnet can be calculated as:

$$h_m = \frac{\mu_r g}{\frac{B_r.4sin\left(\frac{\rho_{pm}}{2}\right)}{B_g \pi} - 1}, \tag{3}$$

where μ_r is the permeability of the magnet and and g is the length of air gap. The model for separating iron losses can be categorized into three components: hysteresis loss, eddy current loss, and additional loss.

$$p_{Fe} = p_h + p_e + p_a = k_h f B_m^{\alpha} + k_e f^2 B_m^2 + k_a f^{1,5} B_m^{1,5} \tag{4}$$

In this design, the additional loss, which accounts for a small portion of the motor iron loss [15], is disregarded. The motor design in this paper utilizes the M530A-50A (European standard EN 10106-1996) non-oriented electrical steel. For the non-oriented model, the parameter α ranges from 1.6 to 1.8, while the values of k_h and k_e for the M530A-50A steel can be found in [16].

The iron loss encompasses the total loss occurring in the stator, rotor, and teeth of the motor. It can be calculated using the loss separation method, as follows:

$$P_{Fe} = p_{stator} M_{stator} + p_{rotor} M_{rotor} + p_{tooth} M_{tooth}. \tag{5}$$

As previously mentioned, the PMSM is excited by permanent magnets instead of excitation currents, resulting in the absence of copper loss in the rotor. Therefore, the copper loss in the PMSM is solely attributed to the stator winding. The calculation for copper loss is as follows:

$$P_{Cu} = Q_s I^2 R, \tag{6}$$

where Q_s is the number of slots, I is the phase current and R is the resistance of the winding in each tooth.

The total loss is the sum of the iron loss and the copper loss, which is given as below:

$$P_{loss} = P_{Fe} + P_{Cu} \tag{7}$$

3. Optimization method

The diagram of the optimization process using genetic algorithm is presented as:

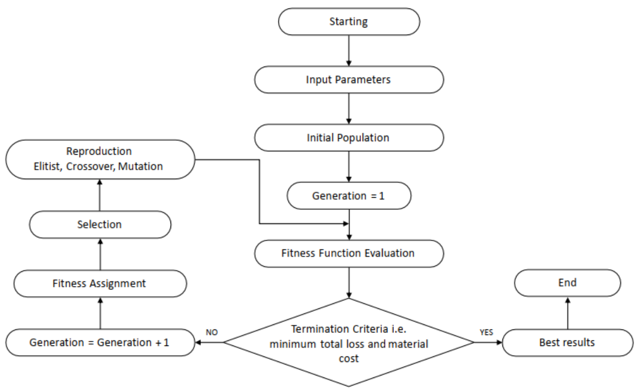

Figure 1. Main steps of a multi-objective genetic algorithm.

The optimization of Permanent Magnet Synchronous Motors (PMSMs) involves a multi-objective problem with numerous variables and constraints. The selection of variables is critical as it directly impacts the output results. In this study, a careful consideration led to the inclusion of seven variables in the optimization process. These variables include the inner stator diameter (y_1), air gap length (y_2), height of the stator yoke (y_3), height of the rotor yoke (y_4), width of the tooth (y_5), current density (***j***), and the number of turns per tooth (n). The variables y_1, y_3, y_4, and y_5 are associated with iron loss and steel volume, whereas y_2, ***j***, and n pertain to magnet dimensions and copper loss. All seven of these variables have the potential to influence both the motor's dimensions and its losses, ultimately leading to variations in the objective functions. Table 1 provides the upper and lower boundaries for each variable:

Table 1. Upper and lower boundaries of optimization variables.

Variable	Lower boundary	Upper boundary
y_1 (mm)	130	150
y_2 (mm)	0,7	1
y_3 (mm)	15	25
y_4 (mm)	15	25
y_5 (mm)	10	15
j (A/mm^2)	2	3,5
n (turns)	75	100

The proposed constraints must be precisely formulated in order to ensure that the optimization results meet all the operational requirements of the Permanent Magnet Synchronous Motor (PMSM). This research paper focuses on three parameters, namely the stator volume, rotor volume, and magnet volume, each accompanied by an equality constraint. The winding's slot fill factor is maintained within the range of 0.45 to 0.55. Additionally, references [17]-[20] provide a typical range for the flux density values of the stator yoke, rotor yoke, and tooth of the PMSM, resulting in four inequality constraints.
The objective functions must be established, specifically the minimization of total loss (P_{loss}) and material cost (C). The material cost encompasses the expenses associated with electrical steel, copper, and magnets, which can be described as follows:

$$C = c_{Fe}M_{Fe} + c_{Cu}M_{Cu} + c_m M_m = c_{Fe}(M_{stator} + M_{rotor} + M_{teeth}) + c_{Cu}M_{Cu} + c_m M_m, \quad (8)$$

where c_{Fe}, c_{Cu}, c_m are the cost per kilogram of electrical steel, copper, and magnet respectively. The mass of the different parts of the motor in (8) is calculated as:

$$M_{stator} = K_1 . \frac{4K_2 y_1 y_3 - 4y_3^2}{x_1^2} \quad (9)$$

$$M_{rotor} = K_1 \frac{(y_1 - 2K_3 y_2)^2 - (y_1 - 2.K_4 y_2 - 2y_4)^2}{y_1^2} \quad (10)$$

$$M_{teeth} = \frac{K_1}{x_1^2} . \left[\frac{\pi}{4}(K_2 y_1 - 2y_4)^2 - Q_s \left(\left(\frac{K_2 - 1}{2} y_1 - y_3 - K_5 \right) \left(\frac{K_2 + 1}{2} y_1 - \frac{K_7}{K_5} y_3 - y_5 + K_7 \right) + K_8 + \frac{h_w}{2} \left(\frac{K_7}{K_5} y_1 - y_5 \right) \right) \right] \quad (11)$$

$$M_{Cu} = \frac{K_{10}}{x_6} . 2\boldsymbol{j} \left(y_5 + \frac{V_{rotor}}{x_1^2} + \frac{K_9}{\sqrt{n}} \mathrm{ceil} \left(\frac{y_7}{\mathrm{floor}\left(\frac{\left(\frac{K_2 - 1}{2} y_1 - y_3 - K_5 \right) \sqrt{1 + a_1^2}}{K_9} \sqrt{n} \right)} \right) \right) \quad (12)$$

$$M_m = 10 \gamma_m V_m . 10^{-9}. \quad (13)$$

Where the factors K_1, K_2, K_3, K_4, K_5, K_6, K_7, K_8 and K_9 are respectively given as:

$K_1 = \frac{\pi}{4} . 10^{-9} \gamma_{Fe} V_{rotor}$, $K_2 = \sqrt{\frac{V_{stator}}{V_{rotor}}}$, $K_3 = \frac{\mu_r}{\frac{B_{rm}}{B_m} - 1} + 1$,
$K_4 = \frac{1}{4}(K_2^2 - 1) - \frac{K_2 + 1}{2} . K_5$, $K_5 = h_w + h_{so}$,
$K_7 = \frac{\pi K_5}{Q_s}$, $K_8 = h_{so} b_{so} + \frac{1}{2} h_w b_{so} + \frac{\pi h_w K_5}{Q_s}$, $K_9 = 1,095\sqrt{\frac{4I}{\pi}}$, $K_{10} = \frac{\gamma_{Cu}.I}{10^{-6}}$.

The other papermeters V_{stator}, V_{rotor}, V_m, B_{rm}, B_m, h_w, h_{so}, b_{so}, γ_{Fe}, γ_{Cu} and γ_m represent the volume of stator, rotor, magnet, the operating remanence of the magnets at working temperature, the flux density above the magnets, the wedge height, the tooth tip depth, the opening width of the semi-closed slot; the mass density of electrical steel, copper, and magnet respectively.
The cost function becomes:

$$C = f_1(x) = f_1(y_1, y_2, y_3, y_4, y_5, y_6, y_7) \quad (14)$$

The loss component parts of each part of the core is calculated as:

$$p_{stator} = \frac{K_{11}}{(y_2 y_3 y_1^{-2})^{1,6}} + \frac{K_{12}}{(y_2 y_3 y_1^{-2})^2}, \quad (15)$$

$$p_{rotor} = \frac{K_{11}}{(y_2 y_4 y_1^{-2})^{1,6}} + \frac{K_{12}}{(y_2 y_4 y_1^{-2})^2} \quad (16)$$

$$p_{tooth} = \frac{K_{13}}{(y_2 y_5 y_1^{-2})^{1,6}} + \frac{K_{14}}{(y_2 y_5 y_1^{-2})^2}, \quad (17)$$

where:

$K_{11} = k_h f \left(\frac{B_m V_m (K_3 - 1)}{2 V_{rotor} k_j} . 10^{-6}\right)^{1,6}$,

$K_{12} = k_e f^2 \left(\frac{B_m V_m (K_3 - 1)}{2 V_{rotor} k_j} . 10^{-6}\right)^{2}$,

$K_{13} = k_h f \left(\frac{\pi B_m V_m (K_3 - 1)}{Q_s V_{rotor} k_j} . 10^{-6}\right)^{1,6}$,

$K_{14} = k_e f^2 \left(\frac{\pi B_m V_m (K_3 - 1)}{Q_s V_{rotor} k_j} . 10^{-6}\right)^{2}$.

The parameters f and k_j are the frequency stacking factor of the iron lamination, respectively.

The resistance of the winding in each tooth is given as below:

$$R = 2K_{15} \boldsymbol{j} n \left(y_5 + \frac{V_{rotor}}{y_1^2} + \frac{K_9}{\sqrt{n}} ceil \left(\frac{x_7}{\text{floor}\left(\frac{\left(\frac{K_2 - 1}{2} y_1 - y_3 - K_5\right)\sqrt{1 + a_1^2}}{K_9} \sqrt{n} \right)} \right) \right) \quad (18)$$

where $K_{15} = \frac{\rho_{Cu}}{I.10^{-3}}$ and ρ_{Cu} is the electrical resistivity of copper. The minimum of total loss means the maximum efficiency. By combining equations (5), (6), (7) together, the total loss function becomes:

$$P_{loss} = f_2(x) = f_2(y_1, y_2, y_3, y_4, y_5, y_6, y_7) \quad (19)$$

4. Numerical and optimal results

The test problem is a practical SPMSM given in Table 2.

Table 2. Main parameters of the SPMSM.

Parameter	Value	Unit
Rated Power	2200	W
Terminal voltage	380	V
Number of slots	12	Slot
Number of pole pairs	5	Pole
Rated speed	600	rpm

The distribution of flux density (**B**) on the stator and rotor before optimization (*top*) and after optimization (*bottom*) is pointed out in Figure 2. It can be seen that before optimization, the value of **B** is observed to be 2.185 (T), which subsequently increases to 2.208 (T) after the optimization process. This means that there is a slight increase in the flux density on the tooth, but the total loss decreased as a result. This change will not have any adverse effects on the motor's operational parameters.

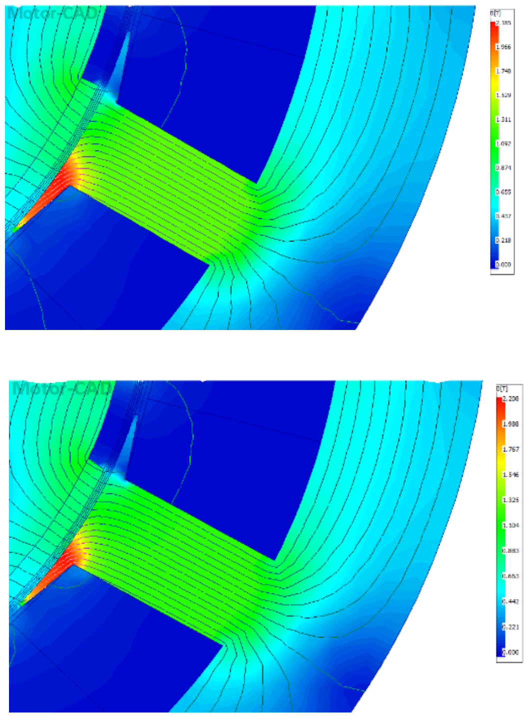

Figure 2. Flux density distribution on the stator and rotor before optimization (*top*) and after optimization (*bottom*).

The distribution of cogging torque for two different cases (before and after optimizations) is shown in Figure 3. The average cogging torque demonstrated a favorable decrease of 1.34 Nm, declining from 3.1 Nm to 1.76 Nm. This outcome aligns with the desired result of reducing cogging torque. Figure 4 presents the distribution of the back EMF. Upon optimization, the root mean square (rms) value of the back electromotive force (EMF) decreased by 2.8V, going from 317.7V to 314.9V. Nevertheless, both values, both before and after optimization, remained smaller than the terminal voltage of 380V. Hence, the operational performance of the motor will not be impacted by this change. The torque characteristic is given in Figure 5. It shows that the optimization process, the motor's torque output exhibited smoother performance, resulting in a reduction in torque ripple as previously mentioned. The average torque output experienced a slight decline from 35.28 Nm before optimization to 35.02 Nm after optimization. However, it remained slightly higher than the desired value. By controlling the advanced phase angle, we were able to increase the torque output back to its pre-optimized level.

The pareto front plot of the objective functions is also presented in Figure 6. It is evident that the two objective functions exhibited inverse changes, indicating that a smaller total loss corresponded to a larger material cost, and vice versa. By examining the scatter plot of the Pareto front, we selected the minimum value for the sum of the two objective functions as the basis for calculating the motor parameters.

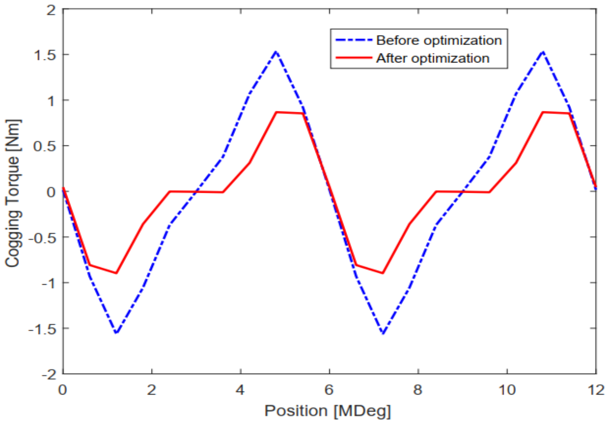

Figure 3. Distribution of cogging torque for two different cases: before and after optimizations

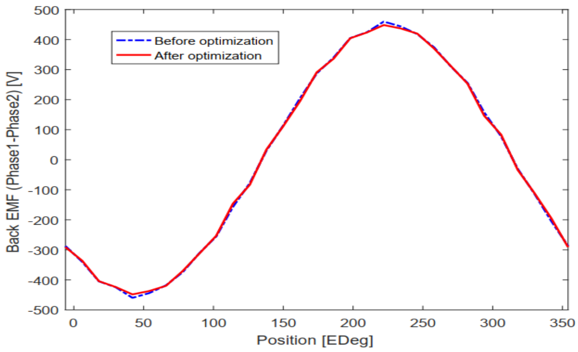

Figure 4. Distribution of the back EMF two different cases: before and after optimizations.

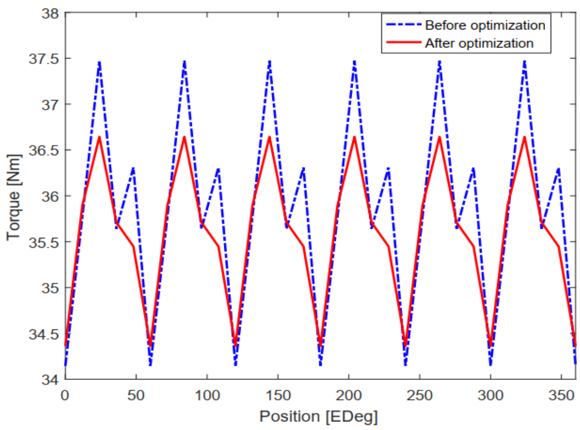

Figure 5. Distribution of the torque two different cases: before and after optimizations.

The optimization results on main parameters of the SPMSM is given in Table 3. The torque ripple percentage decreased by 2.82%, going from 9.26% to 6.44%. Additionally, the motor's efficiency improved from 94.298% to 94.835%. The power factor remained relatively stable, while the total material cost decreased from 358.02$ to 342.8$. Furthermore, the torque output becomes smoother after optimization, indicating a decrease in torque ripple. Although there is a slight increase in the flux density on the tooth, it does not adversely affect any motor parameters during operation. These positive outcomes highlight the favorable comparison between the optimized design and the original configuration.

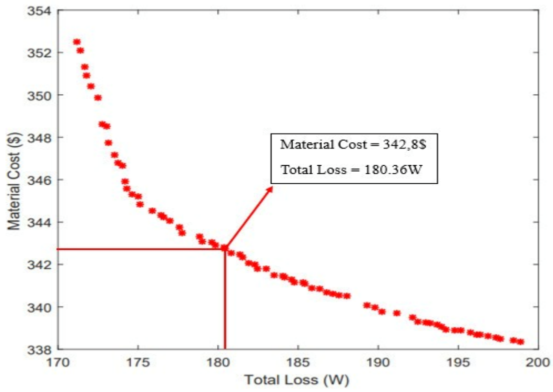

Figure 6. Pareto front results.

Table 3. Optimization results on main parameters of the SPMSM.

Parameter	Before optimization	After optimization
Stator outer diameter (mm)	221.8	218.12
Stator inner diameter (mm)	135	133
Tooth width (mm)	12.3	13.4
Slot height (mm)	23	24
Magnet thickness (mm)	2.45	2.45
Magnet electrical angle	126	122
Active length of iron core (mm)	134	138.6
Number of turns	85	81
Conductor diameter (mm)	1.55	1.64
Slot fill factor	0.52	0.55
Torque Ripple (%)	9.26	6.44

Power factor	0.93	0.93
Shaft torque (Nm)	35.3	35
Efficiency (%)	94.3	94.8
Material cost ($)	358	342.8

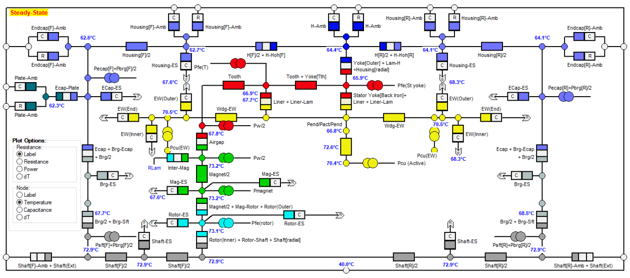

Figure 7. Thermal equivalent circuit after optimization.

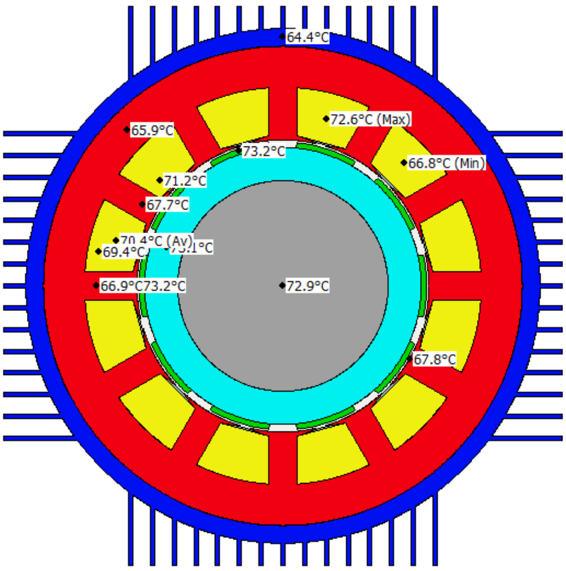

Figure 8. Radial view result of the thermal model after optimization.

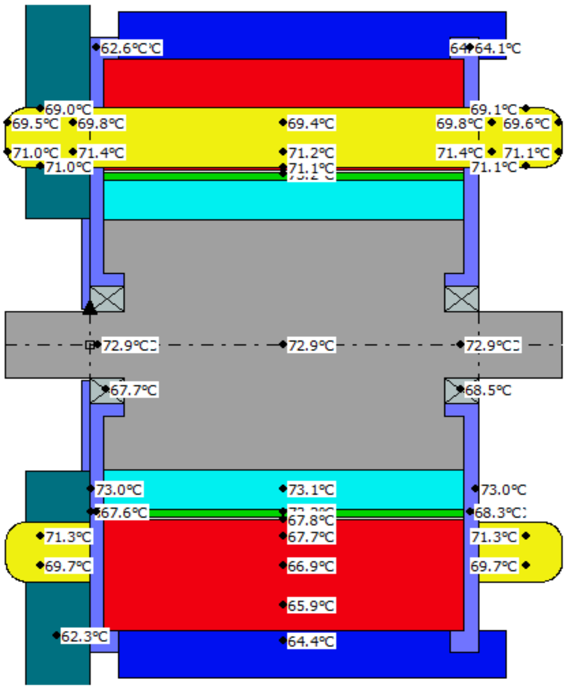

Figure 9. Axial view result of the thermal model after optimization.

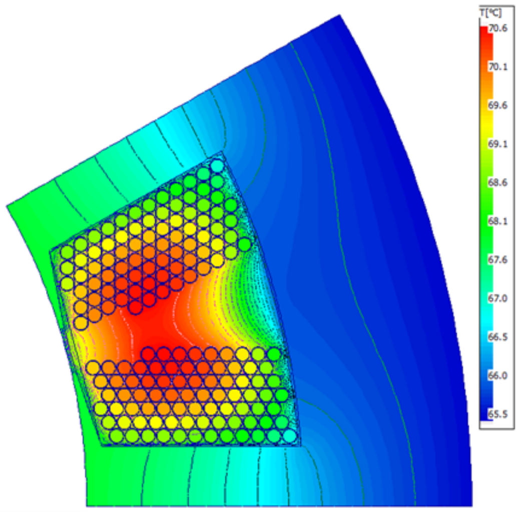

Figure 10. Temperature distribution in the stator slot after optimization.

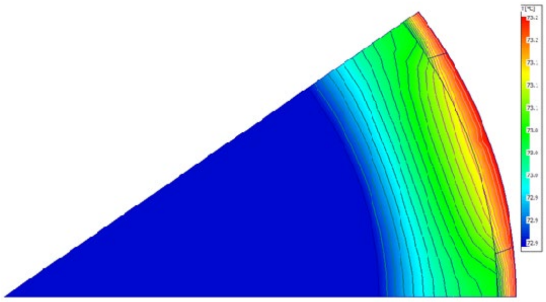

Figure 11. Temperature distribution in the rotor and PM after optimization.

The model of thermal equivalent circuit after optimization is presented in Figure 7. Figures 8 and 9 show the radial and axial view results of the thermal model after optimization already gien in Figure 7. The Temperature distributions in the stator slot and in in the rotor and PM after optimization are pointed out in Figures 10 and 11. Based on the obtained results from Figure 7 to Figure 11, the maximum temperature of the motor is reduced from 78. 4ºC to 73.2ºC due to a reduction of the total losses. Although these two values of the maximum temperature are both still in the safe threshold for the operation of the motor, but they once again demonstrate the correctness and effectiveness of the motor optimization model.

5. Conclusion

This research paper focuses on the design of a SPMSM using a multi-objective optimization approach that incorporates a genetic algorithm. The dimensions of a 2.2 kW SPMSM with a fractional-slot concentrated winding were computed. The main objective of the optimization process was to minimize two crucial factors: total loss and material cost. To validate the effectiveness of the selected variables and constraints in the optimization method, the motor's efficiency was evaluated using the FEM. The results obtained indicate that the optimized design significantly reduces material costs compared to the original design while maintaining the desired efficiency level, but it also brings about desirable changes in other parameters such as cogging torque and torque ripple. Future work could involve the development and optimization of additional goal functions, such as torque output, cogging torque, and torque ripple. Other optimization methods such as particle swarm optimization, cultural algorithm, bee algorithm, and more, could be attempted to tackle the optimization problems and achieve even better results.

Acknowledgements

This research is funded by Hanoi University of Science and Technology (HUST) under project number T2022-PC-008.

References

[1] D. Z. Z. J. ZHANG Haifeng, “Optimization Design and Analysis of Permanent magnet synchronous motor based on VC,” International Conference on Electrical Machines and Systems (ICEMS), 2017 20th.

[2] S. D. S. Jonathan Michael Crider, “An Inner Rotor Flux-Modulated Permanent Magnet Synchronous Machine for Low-Speed High-Torque Applications,” IEEE Transactions on Energy Conversion, Volume 30, Issue 3, September 2015.

[3] S. Y. F. Z. S. J. Y. S. Lishuai Feng, “Study on performance of low-speed high-torque permanent magnet synchronous motor with dynamic eccentricity rotor,” The 2nd International Conference on Power Engineering (ICPE 2021), Nanning, Guangxi, China, December 09–11, 2021.

[4] L. Qinghua, “ANALYSIS, DESIGN AND CONTROL OF PERMANENT MAGNET SYNCHRONOUS MOTORS FOR WIDE-SPEED OPERATION,” Doctoral Thesis, DEPARTMENT OF ELECTRICAL ENGINEERING, NATIONAL UNIVERSITY OF SINGAPORE, 2005

[5] Y.-D. C. J.-H. C. S.-U. C. P.-W. H. D.-H. K. Un-Jae Seo, “General Characteristic of Fractional Slot Double Layer Concentrated Winding Synchronous Machine,” Journal of Electrical Engineering and Technology, March 2013.

[6] P. S. M. N. J. H. Jussila, “Guidelines for Designing Concentrated Winding Fractional Slot Permanent Magnet Machines,” 2007 International Conference on Power Engineering, Energy and Electrical Drives, 12-14 April 2007.

[7] S. S. M. D. Sushruta Mishra, “Genetic Algorithm: An Efficient Tool for Global Optimization,” Advances in Computational Sciences and Technology, ISSN 0973-6107 Volume 10, Number 8 (2017) pp. 2201-2211, 2017

[8] L. P. Goga Cvetkovski, “Multi-objective Optimal Design of Permanent Magnet Synchronous Motor,” 2016 IEEE International Power Electronics and Motion Control Conference (PEMC), Varna, Bulgaria.

[9] J. Gao, L. Dai và W. Zhang, “Improved genetic optimization algorithm with subdomain model for multi-objective optimal design of SPMSM,” CES Transactions on Electrical Machines and Systems, Volume: 2, Issue: 1, March 2018.

[10] L.-Y. L. ,. C.-T. L. P.-L. Chang-Chou Hwang, “Optimal Design of an SPM Motor Using Genetic Algorithms and Taguchi Method,” IEEE TRANSACTIONS ON MAGNETICS, VOL. 44, NO. 11, November 2008.

[11] M. A. J. C. P. V. S. J. S. S. S. M. E. H. A. R. A. Maruthachalam Sundaram, “Design and FEM Analysis of High-Torque Power Density Permanent Magnet Synchronous Motor (PMSM) for Two-Wheeler E-Vehicle Applications,” International Transactions on Electrical Energy Systems, 2022.

[12] T. T. EI KYAW AUNG NAY TUN, “Design of Conventional Permanent Magnet Synchronous Motor used in Electric Vehicle,” International Journal of Scientific Engineering and Technology Research, ISSN 2319-8885, Vol.03,Issue.16, Pages 3289-3293, July 2014.

[13] X. Z. L. Q. Y. D. Weiwei Gu, “ Design and Optimization of Permanent Magnet Brushless Machines for Electric Vehicle Applications,” Energies 2015, 8, 13996–14008.
[14] H. Liu, “Design of High-Efficiency Rare-Earth Permanent Magnet Synchronous Motor and Drive System,” Doctoral Thesis, University of Central Florida, 2015.
[15] M. L. Y. Z. H. W. C. G. Guangwei Liu, “High-Speed Permanent Magnet Synchronous Motor Iron Loss Calculation Method Considering Multi-Physics Factors,” IEEE Transactions on Industrial Electronics, Volume: 67, Issue: 7, July 2020.
[16] W. A. Pluta, “Core loss models in electrical steel sheets with different orientation,” PRZEGLĄD ELEKTROTECHNICZNY (Electrical Review), ISSN 0033-2097, R. 87 No 9b, 2011.
[17] P. Ponomarev, “Tooth-Coil Permanent Magnet Synchronous Machine Design for Special Applications,” Doctoral Thesis, Lappeenranta University of Technology, Lappeenranta, Finland, October 2013.
[18] G. Liu, M. Liu, Y. Zhang, H. Wang and C. Gerada, "High-Speed Permanent Magnet Synchronous Motor Iron Loss Calculation Method Considering Multi-Physics Factors," IEEE Transactions on Industrial Electronics, Volume: 67, Issue: 7, July 2020.
[19] W. A. Pluta, "Core loss models in electrical steel sheets with different orientation," PRZEGLĄD ELEKTROTECHNICZNY (Electrical Review), ISSN 0033-2097, R. 87 No 9b, 2011.
[20] P. Ponomarev, "Tooth-Coil Permanent Magnet Synchronous Machine Design for Special Applications," Doctoral Thesis, Lappeenranta University of Technology, Lappeenranta, Finland, October.